SCIREA Journal of Geosciences

http://www.scirea.org/journal/Geosciences

October 15, 2016

Volume 1, Issue1, October 2016

Evaluation of Land Surface Temperature and Vegetation Relation Based on Landsat TM5 Data

Gulcan Sarp

Department of Geography, Suleyman Demirel University, 32260 Isparta, Turkey,

Email: gulcansarp@sdu.edu.tr

Abstract

Vegetation coverage has a significant role on the Land Surface Temperature (LST) distribution. Remote sensing technologies use the thermal infrared region of the electromagnetic spectrum in order to observe LST. In this paper spatial and temporal distribution of vegetation coverage, land surface temperature investigated, and the relationships among these factors are discussed. In the study LST values were derived from the thermal band of the Landsat 5 Thematic Mapper (TM). Vegetation cover of the test area was derived from the near-infrared and red bands of the Landsat 5 TM by using Normalized Difference Vegetation Index (NDVI). The spatial relationship between LST and NDVI was tested using Getis-Ord Gi* statistics.

The results of the study reveal that vegetation cover was mostly influenced by the LST. The findings showed that in the study area, LST and the NDVI indicates the opposite spatial distribution, indicating that an increase in vegetation abundance would generally reduce surface temperatures.

Keywords: Land surface temperature; Vegetation indices; Thermal remote sensing.

Introduction

Land surface temperature (LST) is defined as how hot the "surface" of the Earth would feel to the touch in a specific location. There are various techniques used for the LST as mobile sampling of air and surface kinetic temperatures from ground and airborne vehicles, and the remote measurement of LSTs from space-borne platforms. However, remote sensing is accepted as one of the most valuable tools for identifying thermal variations within urban settings due to the capability of this tool to collect scores of spatially contiguous samples over large areas instantaneously [2]. Moreover, the remote sensing technique can offer LST measurements concerning the spatial extent of surface heat island effects for metropolitan areas as well as regarding the magnitude of surface temperatures [3]. In this perspective, the spatial resolution of remote sensing thermal data can be defined as the average temperature of surface existing features represented on pixel scale that delineate the changes in emissivity of the land surface [1].

Temperature is one of the major influences on vegetation grown. Conversely, plants influence how hot the surface of the land can become. LST estimation by using the Thermal Infrared Region (TIR) and NDVI studies by using visible and near-infrared portion of the EMS were carried out by many researchers [4, 5, 6, 7]. LST is a significant parameter to determine the energy exchange between the surfaces of the earth [8, 9] and the radiant temperature that will help to understand the change of the surface temperature. NDVI can analyze the temporal and spatial vegetation cover changes over the study region to visualize the variation in the concentration of temperature radiant with respect to time. LST-NDVI assessed through satellite derived products and defines their relationship through conventional statistical method [10, 11]. NDVI not only maps the occurrence of vegetation on a pixel basis, but also offers measures of the quantity or condition of vegetation within a pixel. LST is a valuable indicator of the energy balance at the Earth's surface because it is one of the significant parameters in the physics of land-surface processes on local and global scales [12]. This paper explores the spatial and temporal relationship between LST and NDVI over the Southwest of the Turkey during the summer growing season. On the basis of satellite data analysis, the thermal band derived LST values are compared with NDVI values to reveal the negative correlation between them.

Study area and data

The study area is located at the Southwest of the Turkey as shown in Fig. 1. The study area is characterized by variety of its natural terrain, including plains, lakes, mountains and valleys (Figure 2). The image data used in this study were taken from19 June 2009 for Landsat 5 TM, (path 178, row 034). The satellite image has seven spectral bands with a spatial resolution of 30 meters (Bands 1 to 5 and 7) and 60 meters (Band 6 (thermal infrared)). The sub-scenes of the data were all free of clouds. These images were downloaded freely from Global Land Cover Facility web page (http://glcf.umd.edu/data/landsat/).

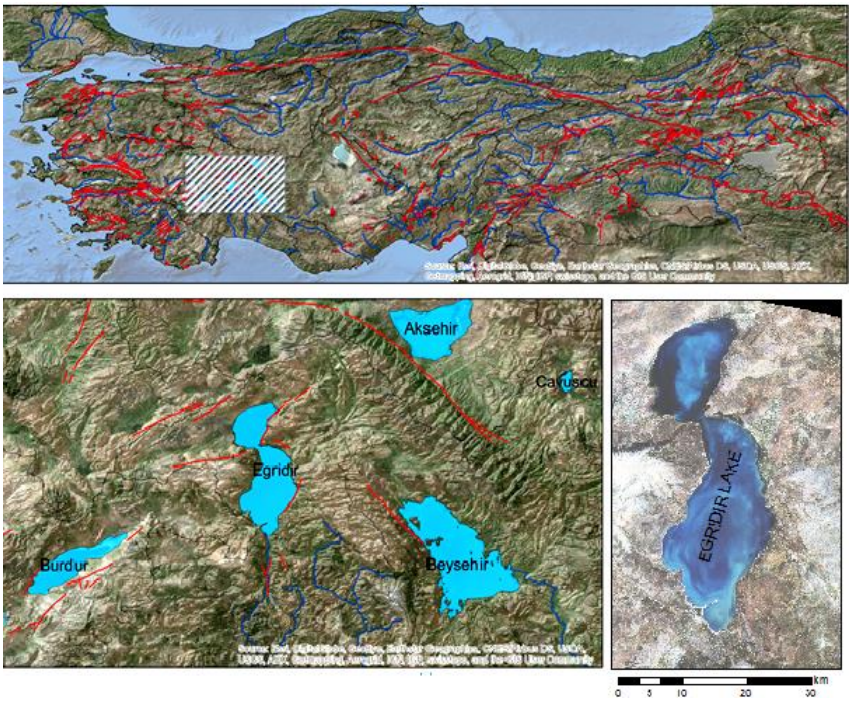

Figure 1. Location of study area

The Proposed Method

The method of the study contains of the processing of the image data to extract LST and NDVI, the integration and evaluation of the LST and NDVI results with the spatial analysis.

1. Land surface temperature extraction from thermal band

In this study, LST were derived from thermal band of the Landsat TM5 satellite image. For Landsat images GeoTIFF with Metatdata format, it was required to transform these data to radiance values. The following formula was used to convert DN's to spectral radiance [13].

$$L_{\lambda} = \frac{(LMax_{\lambda} - LMin_{\lambda})}{(QCalMax_{\lambda} - QCalMin)} X(DN - QCalMin) + LMin_{\lambda} \quad (1)$$

Where; Lʎ is the spectral radiance at the sensor's aperture in W/(m2 sr μm) ;

DN is the quantized calibrated pixel value, *Lmin* and *Lmax* are the minimum and maximum spectral radiance of thermal band respectively, *QCalMin* and *QCalMax* are the minimum and maximum quantized calibrated pixel value in DNs, respectively [14, 20].

In the next step the radiance brightness is converted to temperature in Kelvin using the following equation.

$$T = \frac{K_2}{ln\left(\frac{K_1}{L_{\lambda}}\right)+1} \quad (2)$$

Where *T* is effective at satellite temperature in Kelvin, *Lʎ* is spectral radiance at the sensors aperture; and *K1* and K2 are thermal band calibration constants. For Landsat 5-TM *K1* and *K2* constants are 607.76 and 1260.56, respectively. *T* values are calculated in Kelvin, and are then transformed to Celsius by using the equation (3).

$$T(℃) = T - 2773\ (K) \quad (3)$$

Where T (^{0}C) is the temperature in Celsius.

2. Calculation of NDVI Values

NDVI is the most common method to produce vegetation maps from remote sensing image data. The NDVI is calculated using the ratio between the red and near infrared bands because of the reverse relationship between vegetation brightness in the red and infrared region of the EMS. The TM bands 3 (Red) and 4 (NIR) are used to generate NDVI. The NDVI is derived from TM bands by using given equation;

$$NDVI = (NIR - Red)/\ (NIR + Red) \quad (4)$$

The resulted NDVI values range from –1 to +1. High values indicate active vegetation, and low (near-zero or negative) values indicate other types of materials [15].

3. Determination of the spatial relation between LST and NDVI using. Getis-Ord Gi* statistics

The first law of geography states that ‘‘everything is related to everything else, but near things are more related than distant things’’ [16]. The main principle of spatial autocorrelation (SA) is similar to this law. SA is defined as the correlation of a variable with itself through space

and it tests the assumption of independence. If neighboring areas are similar, then SA is positive. On the other hand, if neighboring areas are dissimilar, then SA is negative and random patterns exhibit no SA. The Getis-Ord Gi* [17, 18, 19] statistic is a local SA index. It is suitable for discriminating cluster structures of hot spots or cold spots concentration which occurs within a defined distance in the whole study area. The Getis-Ord Gi* statistic is calculated using a specified neighborhood distance. If the neighboring feature is within the defined distance of the target feature, then that pair will be assigned a weight of 1; otherwise, the pair will be assigned a weight of 0. High values of the Gi* statistic correspond to hot spots which signify high attribute values located together in a place, while a low value resembles to cold spots representing low values that are located together. The Gi* statistic is calculated using the following equation;

$$G_i^* = \frac{\sum_{j=1} w_{ij} x_j}{\sum_{j=1} x_j} \tag{5}$$

Where; Gi* is the SA statistic of an event i over n events. The term, xj describes the magnitude of the variable x at events j over all n; the CSI at a specific place. The distribution of the Gi* statistic is normal when normality is observed in the underlying distribution of the variable x. In this study the threshold distance was set to zero to indicate that all features were considered neighbors of all other features. This threshold value was applied over the whole region of the study. The output of the Gi function is a z-score for each feature. The standardized Gi* is essentially a z- score and can be linked with statistical significance as;

$$Z(G_i^*) = \frac{\sum_{j=1}^{n} w_{ij} x_j - \bar{x} \sum_{j=1}^{n} w_{ij}^2}{s \sqrt{\frac{n \sum_{j=1}^{n} w_{il}^2 - (\sum_{j=1}^{n} w_{ij})^2}{n-1}}} \tag{6}$$

The outcomes of z-scores highlight the cluster areas spatially where features with either high or low values. A feature with a high value is interesting but may not be a statistically significant hot spot. To be a statistically significant hot spot, a feature will have a high value and be surrounded by other features with high values as well. The local sum for a feature and

its neighbors is compared proportionally to the sum of all features; when the local sum is very different from the expected local sum, and that difference is too large to be the result of random chance, statistically significant z-score results.

In this study The Getis-Ord Gi* statistics is applied to randomly selected 50 point locations and hot spot and cold spot of LST and NDVI values are interpreted using the Gi_Bin field intervals.

Results

LST is derived from thermal band of the Landsat TM5 (Figure 2.a). The result of the LST and NDVI distribution is given in the Fig. 2b and c, respectively. The LST ranged from 5.50 to 42.59 degree with a mean of 30.23. The warmest temperatures are dark brown, while the coldest temperatures are light purple. Moderate temperatures are depicted in shades of yellow and green (Figure 2b). These reverse relation between LST and NDVI also indicated with the LST and NDVI profile (Figure 3 a, and b). NDVI and LST profile exhibited large geographical variations in, height, shape, and number of peaks, with characteristics determined by vegetation density and surface morphology.

NDVI easily separated vegetated areas from areas with little or no vegetative cover. The results of NDVI values have ranged from -0.082 to 0.44 with a mean of 0.19 (Figure 2c). Spatial variation of NDVI is not only subject to the influence of vegetation amount, but also to topography, slope, solar radiation availability, and other factors (Walsh et al., 1997). In this study NDVI of an area containing dense vegetation will tend to high NDVI values (say 0.3 to 0.8). By contrast, bare soil surface areas will be characterized by rather small positive NDVI values (say 0.1 to 0.2). Spatial variation of NDVI is not only influenced by the amount of vegetation alone, but could also be influenced by the topography and gradient of the land and the availability of radiation from the sun.

Different geometric symbols can be used to represent different classes of variation. In this case proportional circles are used to indicate spatial variation in the attribute over the study area, using the sampled point values. The spatial distribution of LST and NDVI within the study area is shown with proportional symbols in Figure 4a and b. The areas with the highest LST values were concentrated within the northern and north-eastern portions of the study area.

On the other hand; the areas with the highest vegetation levels were concentrated within the southern and south-eastern portions of the study area.

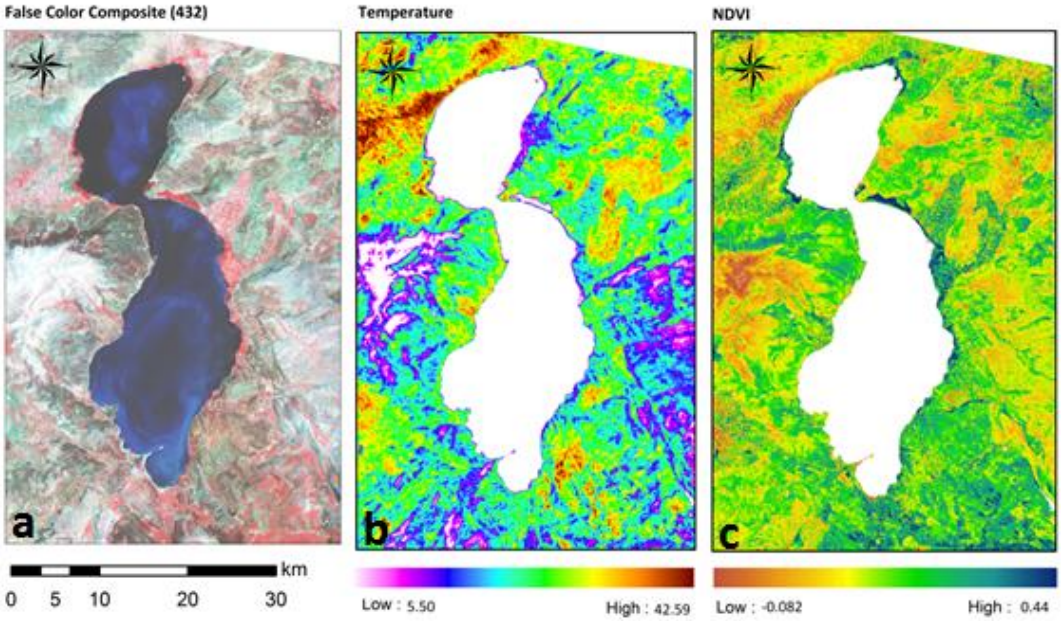

Figure 2. False color composite of Landsat TM (432) (a); LST (b) and NDVI (c) image of the study area.

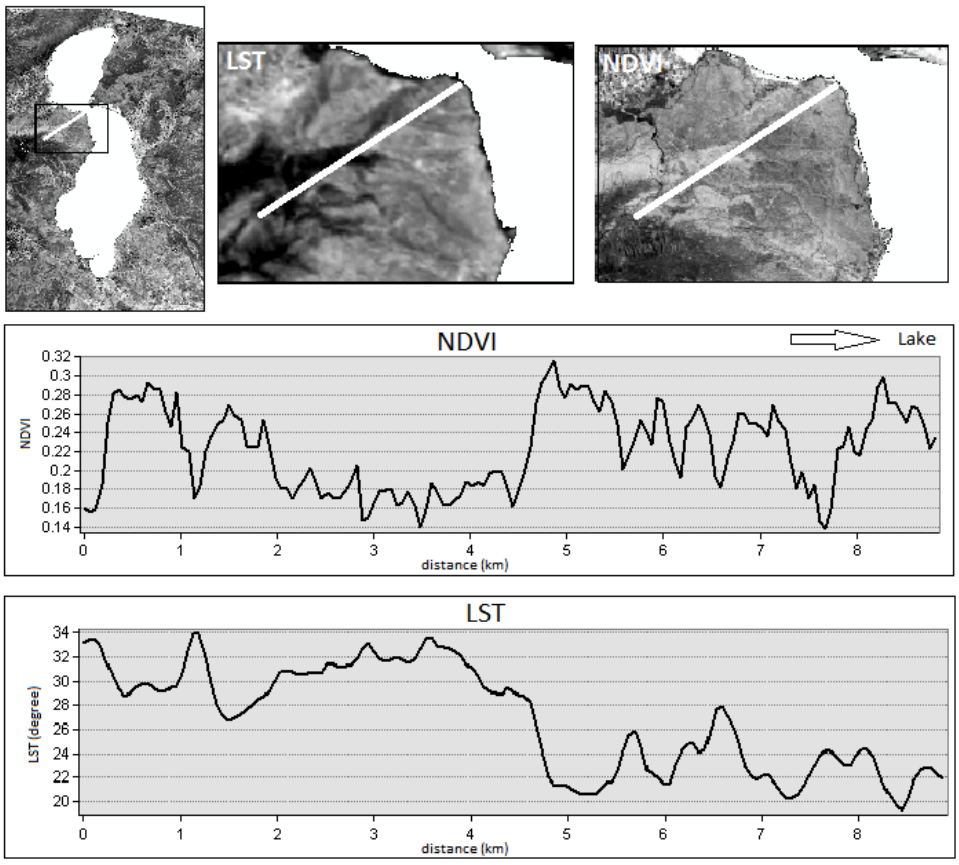

Figure 3. Comparison of NDVI profile with LST profile

The results of the Getis-Ord Gi* reveals statistically significant spatial clusters of high values (hot spots) and low values (cold spots). The Gi_Bin field identifies statistically significant hot and cold spots. Features in the +/-3 bins reflect statistical significance with a % 99 confidence level; features in the +/-2 bins reflect a %95 confidence level; features in the +/-1 bins reflect a % 90 confidence level; and the clustering for features in bin 0 is not statistically significant. According to generated maps of randomly selected 50 data points statistically significant clusters of high and low LST values are placed northwestern and western part of the lake area, respectively. On the other hand, statistically significant clusters of low and high NDVI values are placed in the same area. This result reveals the reverse relation between the LST and NDVI values. In general, the visual pattern of LST was opposite to that of NDVI. The result of the spatial distribution of the LST and NDVI values reveals a strong negative relationship between LST and vegetation cover.

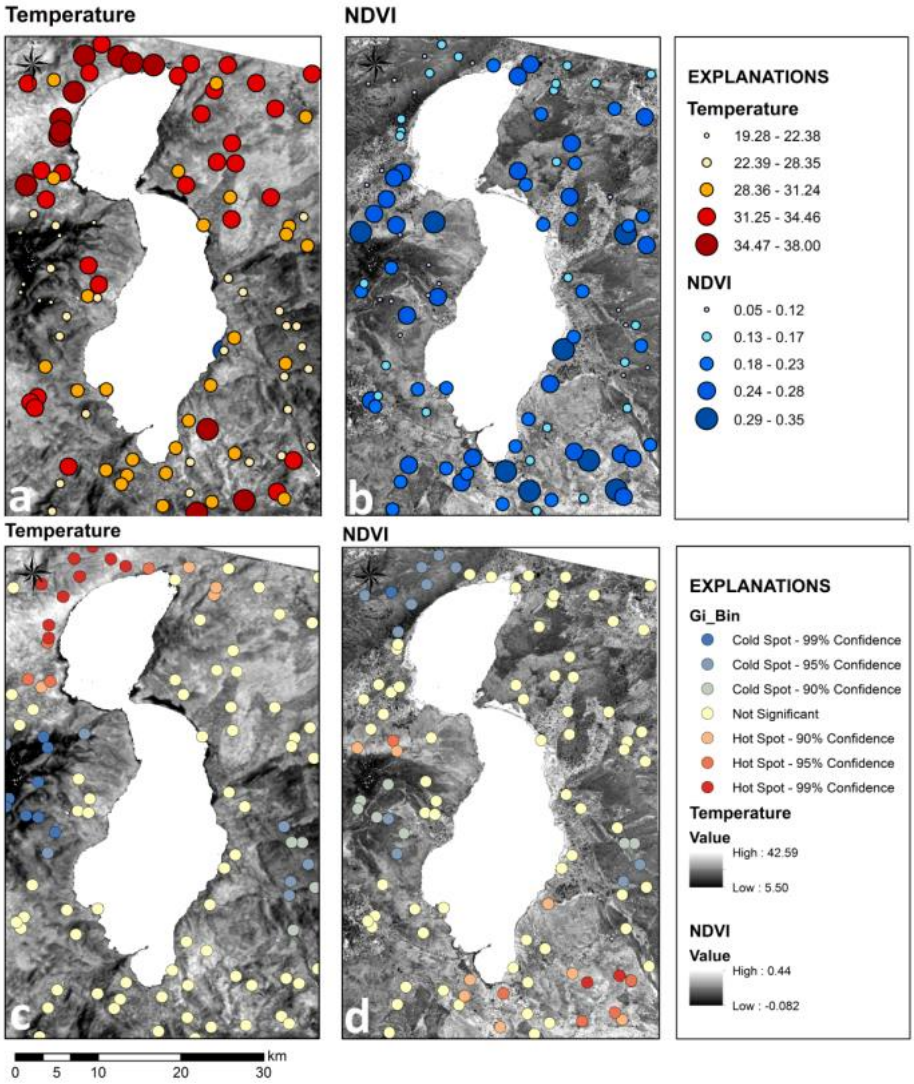

Figure 4. Proportional symbol map of Temperature (a) and NDVI (b)

Conclusions

Vegetation abundance is one of the most influential factors in controlling LST. A wide range of climatic and physical variables affects NDVI, LST, and the relationship between plant cover and temperature. This paper explores the spatial and temporal relationship between LST and NDVI over the Southwest of the Turkey during the summer growing season. On the basis of satellite data analysis, the spatial relationship between LST and NDVI is evaluated using Getis-Ord Gi* statistics. According to results high temperature areas indicate low NDVI values; however, low temperature values are mostly indicated vegetated areas. The results of the Getis-Ord Gi* also reveals the significant inverse relationship between the LST and NDVI values.

References

[1] Anbazhagan S. and Paramasivam C.R., "Statistical Correlation between Land Surface Temperature (LST) and Vegetation Index (NDVI) using Multi-Temporal Landsat TM Data". International Journal of Advanced Earth Science and Engineering, 5 (1): 333-346, 2016.

[2] Yue, W, Xu, J., Tan, W., and Xu, L, "The relationship between land surface temperature and NDVI with remote sensing: application to Shanghai Landsat 7 ETM+ data". International Journal of Remote Sensing, 28, 3205-3226, 2007.

[3] Yuan, F., and Bauer, M.E., "Comparison of impervious surface area and normalized difference vegetation index as indicators of surface urban heat island effects in Landsat imagery". Remote Sensing of Environment, 106, 375-386. 2007.

[4] Valor, E., and Caselles, V. "Mapping Land Surface Emissivity from NDVI: Application to European, African, and South American Areas". Remote Sensing of Environment. 57; 167-184, 1996.

[5] Goetz, S.J. "Multi-Sensor Analysis of NDVI, Surface Temperature and Biophysical Variables at a Mixed Grassland Site". International Journal of Remote Sensing. 18 (1) 71-94, 1997.

[6] Sandholt, I., Rasmussen, K., and Andersen, J. “A Simple Interpretation of the Surface Temperature and Vegetation Index Space for Assessment of Surface Moisture Status”. Remote Sensing of Environment. 79; 213-224, 2002.

[7] Kim, H.M., Kim, B.K., and You, K.S. “A Statistic Correlation Analysis Algorithm between Land Surface Temperature and Vegetation Index” International Journal of Information Processing Systems, 1 (1) 102-106, 2005.

[8] Shah, D.B., Pandya, M.R., Trivedi, H.J., and Jani, A.R. “Estimating Minimum and Maximum Air Temperature Using MODIS Data Over Indo-Gangetic Plain”. Journal of Earth System Science Indian Academy of Sciences, 122 (6) 1593-1605, 2013.

[9] Orhan, O., Ekercin, S., and Filiz Dadaser-Celik. “Use of Landsat Land Surface Temperature and Vegetation Indices for Monitoring Drought in the Salt Lake Basin Area, Turkey”. The Scientific World Journal. 1-11, 2014.

[10] Weng, Q., Lu, D., and Schubring, J. “Estimation of Land Surface Temperature–Vegetation Abundance Relationship for Urban Heat Island Studies”. Remote Sensing of Environmen, 89; 467-483, 2004.

[11] Goetz, S.J. “Multi-Sensor Analysis of NDVI, Surface Temperature and Biophysical Variables at a Mixed Grassland Site”. International Journal of Remote Sensing. 18 (1) 71-94, 1997.

[12] Wan, Z., Wang, P., and Li, X., “Using MODIS Land Surface Temperature and Normalized Difference Vegetation Index products for monitoring drought in the southern Great Plains, USA”. Int. J. Remote Sensing, 25(1): 61–72, 2004.

[13] Chander, G., and Markham, B. “Revised Landsat-5 TM Radiometric Calibration Procedures and Post Calibration Dynamic Ranges”. IEEE Transactions on Geoscience and Remote Sensing. 41 (11) 2674-2677, 2003.

[14] NASA, 2011: Landsat 7 Science Data Users Handbook. Landsat Project Science Office at NASA Goddard Space Flight Centre, Greenbelt, 186 (http://landsathandbook.gsfc.nasa.gov)

[15] Sarp, G., “Determination of Vegetation Change Using Thematic Mapper Imagery in Afşin-Elbistan Lignite Basin; SE Turkey”. Procedia Technology, 1, 407 – 411, 2012.

[16] Tobler, W. R., “A computer movie simulating urban growth in the Detroit region”. Economic Geography, 46: 234–40. 1970.

[17] Mitra, S., “Spatial autocorrelation and Bayesian spatial statistical method for analyzing fatal and injury crash prone intersections”. In Transportation Research Record: Journal of the Transportation Research Board, No. 2136, TRB, Washington, D.C., pp. 92-100, 2009.

[18] Getis, A., Ord, J.K.,. “The analysis of Spatial Association by use of Distance Statistics”. Geographic Analysis, 24 (3), 189-206, 1992.

[19] Ord, J. K., Getis, A., “Local Spatial Autocorrelation Statistics: Distributional Issues and An Application”, Geographical Analysis 27 (4): 286 – 306, 1995

[20] Chander, G. and Markham, B. “Revised Landsat-5 TM Radiometric Calibration Procedures and Postcalibration Dynamic Ranges”. Ieee Transactıons On Geoscıence And Remote Sensıng, 41, (11), 2003.